drones

MDPI

Article

High-Precision Modeling of UAV Electric Propulsion for Improving Endurance Estimation

Xunhua Dai [1,†], Wei Liu [1,†] and Yong Chen [2,*]

[1] School of Computer Science and Engineering, Central South University, Changsha 410083, China; dai.xh@csu.edu.cn (X.D.)
[2] Department of Automation, Central South University, Changsha 410083, China
* Correspondence: chenyong@csu.edu.cn; Tel.: +86-155-7666-3726
† These authors contributed equally to this work.

Highlights

What are the main findings?

- We propose a physics-informed, data-driven framework that integrates dimensional analysis (Buckingham π theorem) with polynomial fitting, enabling high-precision prediction of propeller thrust/power coefficients and motor current under varying inflow conditions.
- The novel torque-based motor current model demonstrates superior accuracy in dynamic airflow compared to conventional thrust-based models, validated across multiple propeller-motor configurations via the UIUC database, a custom test rig, and actual flight tests.

What are the implications of the main findings?

- This modeling framework provides a computationally efficient and accurate tool for UAV propulsion system design and optimization, significantly reducing reliance on extensive experimental data or high-fidelity simulations during the preliminary design phase.
- The improved endurance estimation capability, grounded in reliable torque-current prediction, offers practical benefits for mission planning, energy management, and overall performance enhancement of electric UAVs across diverse operational scenarios.

Abstract

The electric propulsion system is a critical determinant of unmanned aerial vehicles' (UAVs') operational capabilities, particularly endurance performance. This paper proposes a high-precision modeling framework for UAV electric propulsion systems to improve endurance estimation. By integrating dimensional analysis based on the Buckingham π theorem with data-driven parameter fitting, the method accurately predicts propeller thrust, power, and motor current under varying inflow conditions using limited experimental data. The proposed models and complete implementation are publicly available, facilitating reproducibility and further research. The key novelty of this work lies in the tight integration of dimensional analysis (via Buckingham's π theorem) with a data-driven torque-based motor current model, enabling accurate cross-configuration predictions for both propeller aerodynamics and motor electrical characteristics using limited experimental data. The model is rigorously validated against the UIUC propeller database, a custom-built inflow test rig, and actual flight tests. The results demonstrate that the proposed approach achieves superior prediction accuracy across multiple propeller-motor configurations while significantly reducing computational costs. This work provides a reliable foundation for improving UAV endurance estimation and propulsion system design.

Check for updates

Academic Editor: Abdessattar Abdelkefi

Received: 25 November 2025
Revised: 15 January 2026
Accepted: 22 January 2026
Published: 23 January 2026

Copyright: © 2026 by the authors. Licensee MDPI, Basel, Switzerland. This article is an open access article distributed under the terms and conditions of the Creative Commons Attribution (CC BY) license.

Keywords: UAV propulsion; high-precision modeling; improving endurance estimation; Buckingham theorem; electric propulsion

1. Introduction

Table 1 summarizes the primary symbols used throughout this paper. The equivalent current I_e refers to the effective direct current representation of the three-phase alternating current in BLDC motors and serves as the direct parameter for estimating battery energy consumption. The air compressibility factor K and its derived dimensionless parameter B characterize the influence of air compressibility on propeller performance. Other key dimensionless parameters include the thrust coefficient C_T, power coefficient C_P, advance ratio J, and pitch ratio β.

Table 1. Summary of symbols and notation.

Symbol	Description
D	Propeller diameter
P	Propeller pitch
ρ_{air}	Air density
V	Inflow velocity
n	Rotational speed
T	Thrust
Q	Torque
I_e	Equivalent motor current
U	Voltage
C_T	Thrust coefficient
C_P	Power coefficient
C_Q	Torque coefficient
J	Advance ratio
β	Pitch ratio
K	Air compressibility factor
B	Dimensionless compressibility parameter

Accurate endurance estimation through high-precision modeling of electric propulsion systems represents a critical challenge in unmanned aerial vehicle (UAV) development. Electric propulsion systems fundamentally determine UAV performance, directly influencing key operational metrics such as flight endurance, payload capacity, and mission reliability. As UAV applications expand across diverse sectors, including defense [1,2], agriculture [3,4], logistics, and commercial services [5,6], the demand for accurate and improved endurance estimation methods has become increasingly urgent. Current industry practices often rely on empirical "build-and-fly" approaches for propulsion system selection and endurance assessment [7]. These methods are inefficient, costly, and frequently lead to suboptimal system configurations. This limitation is particularly pronounced when addressing diverse propeller geometries and variable inflow conditions encountered during actual operations.

Improving endurance estimation requires advances in propulsion system modeling techniques. Existing approaches fall into two broad categories: physics-based and data-driven methods, each with distinct limitations for practical UAV design. Physics-based models span a wide fidelity spectrum. Low-fidelity methods such as Blade Element Momentum Theory (BEMT) [8–10] and vortex theory [11] offer rapid evaluation but limited accuracy. Medium-fidelity approaches, including prescribed wake and free wake models [12,13], incorporate wake interactions for improved predictions. High-fidelity

Computational Fluid Dynamics (CFD) and Reynolds-Averaged Navier–Stokes (RANS) simulations [14,15] provide detailed results at prohibitive computational costs, often requiring geometric data that are unavailable in early design stages. Recent work by Chen et al. [16] exemplifies medium-fidelity approaches for distributed electric propulsion UAVs, employing the Vortex Lattice Method and Actuator Disk Theory for efficient aerodynamic analysis during overall design phases. However, this approach still requires substantial computational resources for comprehensive system evaluation. Meanwhile, Tofan-Negru et al. [17] demonstrated high-fidelity CFD simulations with sliding mesh techniques for quadcopter propeller flow fields, achieving detailed flow characterization at significant computational expense that limits practical design iteration.

In parallel, data-driven methods have emerged as practical alternatives. Kedarisetty et al. [18] developed quadratic fits using wind tunnel and CFD data for specific propeller sizes. Bryant [19] examined thrust characteristics via CFD for 7-inch propellers. Budinger and Reysset [20] established empirical relationships for APC propellers based on pitch and advance ratio. Kulanthipiyan et al. [21] proposed a comprehensive design framework for small electric UAVs by analyzing 42 existing propulsion systems. They introduced a novel torque factor to determine operating current and voltage, demonstrating significant improvements in current consumption (up to an 84% reduction) and system endurance. However, these empirical models are typically tailored to specific propeller types or limited operational ranges, restricting their generalizability across diverse designs. For motor performance estimation, while comprehensive physical models of Brushless Direct Current (BLDC) motors exist [22–24], they often rely on proprietary parameters that are difficult to measure in practice. Machine learning techniques [25,26] offer alternative pathways but require substantial training data and careful feature engineering.

The persistent challenge lies in developing modeling approaches that balance accuracy, generalizability, and computational efficiency. This is particularly important for improving endurance estimation, which requires reliable performance prediction across varying operational conditions. Physics-based approaches can be computationally prohibitive or data-intensive for early-stage design [16,17], while many data-driven models lack broad generalizability or require substantial training data. This gap is particularly problematic for UAV designers who need to rapidly evaluate multiple propeller–motor combinations under varying inflow conditions with limited experimental resources.

To address this research gap, this paper introduces a high-precision modeling framework that integrates dimensional analysis (via the Buckingham π theorem) with parametric fitting. This approach enables improved endurance estimation through accurate prediction of key propulsion parameters—including propeller thrust, power, and motor current—under varying inflow conditions. The principal contributions of this work are fourfold.

First, we introduce a novel modeling paradigm that seamlessly bridges dimensional analysis and empirical fitting for UAV propulsion systems. This high-precision cross-configuration modeling approach constructs models based on dimensionless parameters, achieving improved prediction accuracy across different propeller geometries and motor types using minimal experimental data. Our method addresses the accuracy limitations of existing empirical models [18,20,21] while avoiding the computational intensity of high-fidelity simulations [17].

Second, the proposed framework enables improved endurance estimation capability through the integration of torque-based motor current modeling with propeller performance prediction. This provides more reliable endurance estimation across varying inflow conditions for UAV mission planning and system optimization.

Third, the model offers computational practicality for design iteration by employing computationally inexpensive polynomial fitting based on dimensionless groups. This closed-form solution facilitates rapid performance evaluation and optimization, presenting advantages over high-fidelity CFD [14,15] or complex medium-fidelity aerodynamic methods [16] during preliminary design stages.

Finally, we conduct comprehensive experimental validation against the public UIUC propeller database, through a custom-built inflow test rig, and actual flight tests. This multi-faceted validation demonstrates performance under both static and dynamic operational conditions, enhancing practical relevance beyond simulation-based studies [16,17].

The remainder of this paper is organized as follows. Section 2 details the propulsion system modeling methodology and its derivation. Section 3 presents validation results, comparing the proposed approach with existing models and conducting comprehensive performance evaluation using experimental datasets. Finally, Section 4 summarizes the key findings and discusses future research directions.

2. Materials and Methods

2.1. Problem Description

Accurately predicting key performance parameters is crucial for UAV propulsion system optimization. The propulsion system estimation problem aims to establish predictive models based on several parameter categories: propeller geometric parameters (diameter D and pitch P), aerodynamic parameters (air density ρ_{air} and incoming flow velocity V), motion parameters (rotational speed n and torque Q), and motor parameters (equivalent current I_e and voltage U).

During UAV flight operations, the propulsion system primarily provides lift and thrust to maintain airborne operations and overcome gravitational forces. The thrust generated by the propeller serves as the principal lifting force, while the motor regulates propeller rotational speed to control thrust magnitude. By accurately modeling the relationship between propeller thrust and motor current, we can predict UAV endurance and flight stability across varying operational conditions. Consequently, the primary output targets include the thrust coefficient C_T, power coefficient C_P, and motor current I_e.

The selection of C_T, C_P, and I_e as key outputs is justified by their distinct roles in propulsion system characterization and endurance estimation. The thrust coefficient C_T, as a dimensionless parameter, effectively captures propeller thrust generation efficiency across different sizes and operating conditions, enabling direct comparison and scaling between propeller designs. The power coefficient C_P characterizes propeller power consumption characteristics, serving as the fundamental input for energy usage analysis and endurance prediction. Motor current I_e directly determines battery energy consumption, making it the most practical parameter for endurance estimation due to its easy measurability during flight tests and direct correlation with system power draw.

The solution objective establishes predictive models for C_T, C_P, and I_e using data-driven methods while satisfying two critical constraints. First, the model should generalize to cross-scenario predictions for different propeller types. Second, the motor current model should maintain compatibility with both static and dynamic incoming flow conditions, achieved by capturing the intrinsic relationship between torque and current to indirectly reflect the impact of varying inflow conditions on motor load and power consumption.

Therefore, the core objective of this paper is to establish a high-precision modeling framework for predicting C_T, C_P, and I_e to significantly improve the reliability of endurance estimation for UAVs under varying inflow conditions. This objective is achieved through two key pathways: (1) enabling cross-propeller configuration performance prediction via dimensional analysis based on the Buckingham π theorem; (2) ensuring prediction accuracy

under both static and dynamic inflow conditions by introducing a torque-based motor current model. The entire modeling workflow, illustrated in Figure 1, is designed to balance accuracy, generalizability, and computational efficiency, as detailed in the following sections.

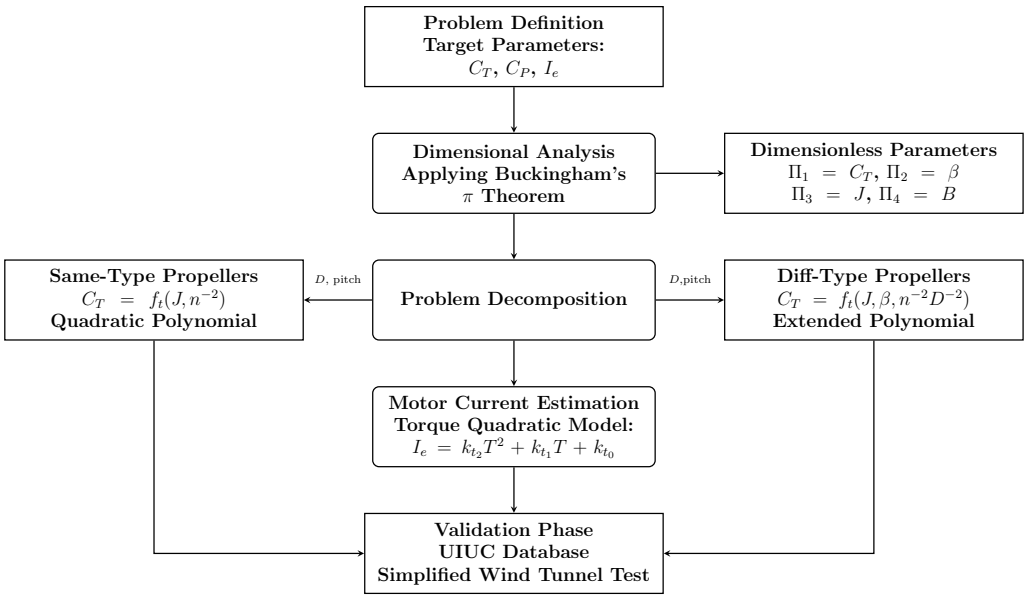


Figure 1. Workflow for parameter prediction based on Buckingham π theorem

2.2. Integrated Experiment-Modeling Framework

To ensure the developed models are both physically consistent and empirically grounded, we have established a closed-loop framework that tightly couples experimental data collection with model development. This integrated approach consists of three synergistic components:

1. Public Wind-Tunnel Database for Static Performance Baseline: The UIUC Propeller Database provides standardized wind-tunnel measurements under controlled static inflow conditions. These data serve as the primary source for establishing the dimensionless relationships between propeller geometry (β), flight state (J), and aerodynamic coefficients (C_T, C_P). The database's rigorous experimental protocols ensure data quality and reproducibility.
2. Custom Inflow Test Rig for Dynamic Performance Characterization: To capture the effects of dynamic inflow on both propeller and motor performance, we designed and constructed a simplified inflow testing apparatus. This rig enables synchronous measurement of propeller thrust (T), torque (Q), power (P_P), motor current (I_e), voltage (U), and rotational speed (n) under controlled horizontal inflow velocities (0–15 m/s). The collected dataset encompasses multiple propeller–motor combinations, providing the necessary empirical foundation for developing and validating the torque-based motor current model.
3. Flight Tests for System-Level Validation: To bridge the gap between component-level models and integrated system performance, we conducted comprehensive flight tests under real-world conditions. These tests provide independent validation data that capture the coupled interactions between propeller aerodynamics, motor electromechanics, and flight dynamics.

This three-tiered validation strategy ensures that each modeling step—from dimensionless parameter derivation to polynomial coefficient fitting—is directly informed by experimental evidence. The UIUC data anchor the propeller models in established aerodynamic

principles; the custom rig data capture dynamic inflow effects critical for motor current prediction; and flight data verify model performance in integrated operational scenarios.

2.3. Theoretical Foundation: Dimensional Analysis and Buckingham π Theorem

Dimensional analysis and the Buckingham π theorem are classic methods in fluid mechanics and propulsion system modeling. The focus of this paper is not to restate the theorem itself, but to systematically demonstrate its application in constructing a practical propulsion system model for multi-rotor UAVs that enables cross-configuration predictions. Specifically, we clarify how to select appropriate subsets of dimensionless parameters derived from the theorem for both same-model and cross-model scenarios, and how to interface these with a motor current model, ultimately serving endurance estimation. This complete workflow is illustrated in Figure 1.

Following the methodology established in [20], propeller thrust can be expressed as

$$\text{Thrust} = f(D, P, \rho_{\text{air}}, K, n, V) \tag{1}$$

It should be noted that Equation (1), closely following the derivation in [20], does not explicitly include the Reynolds number (Re). This implies that the model is applicable under medium-to-high Reynolds number flow conditions ($Re > 10^4$), where viscous forces are secondary to inertial forces. For very small UAVs or micro-propellers operating at extremely low flight speeds, the Reynolds number can be low, and viscous effects may become significant, potentially leading to errors when applying the model.

Similarly, propeller power can be represented as:

$$\text{Power} = f(D, P, \rho_{\text{air}}, K, n, V) \tag{2}$$

where D denotes propeller diameter, P represents propeller pitch, ρ_{air} indicates air density, K signifies the air compressibility factor, n denotes propeller rotational speed, and V represents relative airflow speed. Direct computation using these parameters proves complex, necessitating Buckingham Theorem application for equation simplification. This analysis reduces the seven physical quantities involving three fundamental dimensions to four dimensionless parameters.

For the thrust equation, the final dimensionless parameter combination is

$$\Pi_1 = C_T = \frac{\text{Thrust}}{\rho_{\text{air}} n^2 D^4} \tag{3}$$

$$\Pi_2 = \beta = \frac{P}{D} \tag{4}$$

$$\Pi_3 = J = \frac{V}{nD} \tag{5}$$

$$\Pi_4 = B = \frac{K}{\rho_{\text{air}} n^2 D^2} \tag{6}$$

where C_T represents the propeller thrust coefficient, β denotes the propeller pitch ratio, J indicates the propeller advance ratio, and B signifies the air compressibility factor. (analogous to Mach number M). According to fluid mechanics principles, $K/\rho_{\text{air}} = a^2$, where a is the speed of sound [20]. Consequently, B can be rewritten as

$$B = \frac{K}{\rho_{\text{air}} n^2 D^2} = \frac{a^2}{n^2 D^2} \propto \frac{1}{M_{\text{tip}}^2}$$

where $M_{\text{tip}} = (nD)/a$ is the propeller tip Mach number.

According to the Buckingham π theorem, the thrust equation transforms into a functional relationship between dimensionless parameters:

$$C_T = f_t(\beta, J, B) \tag{7}$$

This parameter prediction workflow based on the Buckingham π theorem is illustrated in Figure 1.

Similarly, the power equation can be reformulated as

$$C_P = f_p(\beta, J, B) \tag{8}$$

In aerodynamic applications, flight speeds below 0.3 Mach are generally considered low-speed regimes where air compressibility effects are negligible. Since conventional UAV flight speeds remain well below this threshold, K can be treated as constant. Furthermore, the relationship between propeller torque coefficient C_Q and power coefficient C_P follows

$$C_Q = \frac{C_P}{2\pi} \tag{9}$$

Accurate estimation of propeller power parameters enables precise determination of propeller torque parameters.

Propeller performance parameter estimation divides into two categories: estimation based on existing same-type data and estimation based on existing different-type data. The subsequent sections analyze both cases and develop corresponding fitting models.

2.4. Single-Propeller Model Parameter Estimation

For identical propeller models, parameters D and P remain constant, and parameter β can, similarly, be treated as constant. Under standard temperature and low-speed conditions, the air compressibility factor K and air density ρ_{air} can likewise be considered constants. Consequently, based on existing data, the parameter estimation equations for identical propeller models simplify to

$$C_T = f_t\left(J, n^{-2}\right) \tag{10}$$

$$C_P = f_p\left(J, n^{-2}\right) \tag{11}$$

To model the functional relationships f_t and f_p, we employ polynomial regression rather than more complex models like neural networks. This selection is justified by several compelling reasons relevant to the engineering context. Polynomial regression offers superior interpretability, computational efficiency, and suitability for limited data scenarios, with established precedent in propeller performance modeling. The closed-form equations provide clear physical interpretation of coefficients, while low computational costs support rapid design iteration. This approach effectively mitigates overfitting risks with sparse experimental data, and prior studies [18,20,27] confirm that low-order polynomials adequately capture C_T and C_P variations with advance ratio J.

Analysis of wind tunnel data for propellers indicates that second-order polynomials effectively apply to propeller parameter estimation:

$$\begin{aligned}\tilde{C}_j = {} & a_{j,00} + a_{j,01} \cdot n^{-2} + a_{j,10} \cdot J \\ & + a_{j,11} \cdot n^{-2} \cdot J + a_{j,20} \cdot J^2,\ j \in [t, p]\end{aligned} \tag{12}$$

The selection of the second-order polynomial form is based on the following comprehensive considerations. First, polynomial coefficients have good physical or empirical

interpretability. Second, to objectively evaluate the impact of model complexity, we conducted a systematic bias-variance analysis. In the cross-model prediction task using the UIUC database (with training and test sets partitioned by propeller model), the average test performance of second-order and third-order polynomials was very close (average test R^2: second-order 0.9755, third-order 0.9759), but the second-order model had lower average test RMSE (second-order 0.0052, third-order 0.0057) and significantly fewer parameters, indicating better generalization ability and lower risk of overfitting. Finally, as shown in literature [18,20,27], low-order polynomials are already sufficient to capture the trends of C_T and C_P with advance ratio J. Therefore, the second-order polynomial strikes an optimal balance between accuracy, simplicity, and generalization capability.

Additionally, we performed a local normalized sensitivity analysis at the training set center point (input variations of ±10%). For the thrust coefficient C_T model, the sensitivity ranking relative to key input parameters is as follows: pitch ratio β (2.13) > advance ratio J (-1.58) > n^{-2} term (-0.16). This indicates that the model output is most sensitive to propeller geometry (β) and flight state (J), while being relatively insensitive to small changes in the inverse square of rotational speed, further validating the physical rationality of the model structure.

2.5. Cross-Propeller Model Parameter Estimation

For different propeller models, parameters D and P are no longer constants, and β should be treated as a variable. Under standard temperature and low-speed conditions, the air compressibility factor K and air density ρ_{air} can be regarded as constants. Consequently, based on existing data, the parameter estimation equations for different propeller models simplify to

$$C_T = f_t\left(J, \beta, n^{-2}D^{-2}\right) \tag{13}$$

$$C_P = f_p\left(J, \beta, n^{-2}D^{-2}\right) \tag{14}$$

It is important to clarify that the functional forms shown in Equations (10) and (11) are practical engineering expressions derived from the complete dimensionless relation $C_T = f_t(\beta, J, B)$ (Equation (7)) for the specific scenario of "same propeller models". The dimensionless parameter $B = K/(\rho_{\text{air}} n^2 D^2)$ characterizes the influence of air compressibility. For a propeller with fixed geometry (D constant) and under low-speed standard conditions (where K and ρ_{air} are approximately constant), the value of B is inversely proportional only to the square of the rotational speed, i.e., $B \propto n^{-2}$. Therefore, in data-driven polynomial fitting, we directly use n^{-2} as an input variable to capture the physical effect represented by B. The proportionality constant $\frac{K}{\rho_{\text{air}} D^2}$ is naturally absorbed into the various coefficients of the polynomial regression. This treatment yields a simpler and more easily fitted expression while maintaining model prediction accuracy. It is essentially a parameterized equivalent representation, whose physical origin remains the dimensionally homogeneous dimensionless relation.

The rationale for polynomial regression extends to the cross-model scenario. Introducing pitch ratio (β) and the combined term ($n^{-2}D^{-2}$) as additional independent variables naturally leads to a multi-variable polynomial formulation. This approach maintains benefits of clarity and computational efficiency while enabling model generalization across different propeller geometries.

Preliminary analysis of the UIUC Propeller Database strongly supports this approach. When performance data from various propellers are plotted in the dimensionless C_T-J-β and C_P-J-β spaces, clear and consistent functional trends emerge across different designs. Although each propeller exhibits unique performance characteristics, these characteristics

overlap and form continuous, predictable landscapes when parameterized by J and β. This observation justifies our unified modeling approach across different propeller models using these dimensionless groups as inputs, with subsequent validation in Section III quantitatively confirming the high prediction accuracy achieved.

Second-order polynomials effectively apply to cross-model parameter estimation:

$$\begin{aligned}\tilde{C}_j = {} & a_{j,000} + a_{j,001} \cdot J + a_{j,002} \cdot J^2 \\ & + a_{j,011} \cdot n^{-2}D^{-2} \cdot J + a_{j,012} \cdot n^{-2}D^{-2} \cdot J^2 \\ & + a_{j,100} \cdot \beta + a_{j,101} \cdot \beta \cdot J + a_{j,102} \cdot \beta \cdot J^2, \\ & j \in [t, p]\end{aligned} \tag{15}$$

2.6. Motor Current Estimation Methodology

UAVs typically employ Brushless Direct Current (BLDC) motors, where current and voltage represent alternating signals that pose measurement and analysis challenges. Consequently, equivalent current and equivalent voltage methods are commonly adopted in research. This study focuses primarily on motor current estimation, with recent research demonstrating the effectiveness of combined electromagnetic and thermal modeling in UAV propulsion systems [28] for precise and robust motor parameter prediction across operating conditions.

Motor current must supply the power required to overcome propeller aerodynamic torque (Q). Previous work, such as [29], proposed a motor current model using thrust (T) as the independent variable:

$$I_e = f_{\Pi}(T) = k_{t_2} \cdot T^2 + k_{t_1} \cdot T + k_{t_0} \tag{16}$$

This model is effective under static or fixed advance ratio conditions where thrust and torque maintain strong correlation for specific propellers. However, under varying inflow conditions (i.e., varying advance ratio J), the relationship between thrust and torque changes significantly. Aerodynamic torque (Q) provides a direct measure of aerodynamic load on the motor and maintains more fundamental linkage to current draw.

Therefore, to develop a model that retains accuracy across varying inflow conditions, we propose using aerodynamic torque (Q) as the independent variable. Analysis of experimental motor data confirms that a quadratic polynomial with respect to torque provides suitable fitting:

$$I_e = f_{Torque}(Q) = k_{q_2} \cdot Q^2 + k_{q_1} \cdot Q + k_{q_0} \tag{17}$$

This torque-current quadratic model is derived from observations of experimental data. It should be noted that Equation (17) implicitly assumes that the brushless DC motors under study have similar electromagnetic designs (e.g., magnetic circuits, winding methods), such that the torque constant K_T maintains an approximately linear relationship with current within the investigated range, and a quadratic polynomial is sufficient to describe nonlinear factors such as losses. For motors with vastly different electromagnetic characteristics (e.g., different series or brands), the coefficients $k_{q_2}, k_{q_1}, k_{q_0}$ may require recalibration.

2.7. Modeling Assumptions and Limitations

To ensure the practicality of the model under typical UAV operating conditions and to clarify its scope of applicability, this study is built upon the following core assumptions:

1. Low-speed incompressible flow assumption: For conventional small UAVs, their flight Mach number is typically below 0.3. Therefore, the air compressibility factor K in the model is treated as a constant, and compressibility effects are neglected.

2. Material and manufacturing consistency assumption: The model derivation implicitly assumes that the propellers involved have similar material properties and manufacturing processes, ignoring aerodynamic performance variations due to material differences or manufacturing tolerances.
3. Uniform steady inflow assumption: The theoretical model is derived based on uniform steady incoming flow. Although the experimental setup in Section 3.3 can provide approximately uniform inflow, turbulent and unsteady effects in real flight are not explicitly considered in the model.

In long-duration missions, endurance prediction errors may accumulate due to ignored environmental variations (e.g., temperature and pressure changes) and inherent model errors. Under high-speed (near-sonic), extreme environmental, or strong turbulent flow conditions, model accuracy may degrade.

3. Results

3.1. Experimental Setup and Dataset Description

This section validates the accuracy of the proposed model using publicly available datasets and a custom-built experimental platform. The validation process comprises three main components: dataset and experimental configuration, including introductions to the UIUC Propeller Database and the simplified wind tunnel test rig design; comparison models and experimental objectives, defining baseline comparison models (ModelA, ModelB) and validation targets; and result analysis, evaluating the accuracy of propeller parameter estimation and motor current estimation followed by discussion of model limitations.

Table 2 provides a comprehensive overview of the validation methodology, detailing the content categories and descriptions for each subsection to ensure systematic evaluation of the proposed modeling framework.

Table 2. Overview of subsection content in VALIDATION.

Subsection	Content Category	Description
Section 3.2	Dataset Description	Introduction to the composition and key parameters of the UIUC database (geometric parameters, performance data).
Section 3.3	Experimental Configuration	Description of the hardware design, test parameters, and data acquisition methods of the self-built test rig.
Section 3.4	Model Description	Comparison of modeling methods
Section 3.5	Experimental Objectives and Results	Validation of SC_T and SC_P estimation accuracy for same-model/different-model propellers (Root Mean Square Error (RMSE) comparison).
Section 3.6	Experimental Objectives and Results	Analysis of motor current model adaptability under static and dynamic airflow conditions.

3.2. UIUC Propeller Database

The UIUC Propeller Database, developed by the aerospace engineering team at the University of Illinois at Urbana-Champaign (UIUC), provides comprehensive experimental data and analysis of propeller performance characteristics. This database contains extensive experimental measurements for various propeller types tested under diverse operating

conditions, making it widely utilized in aerodynamic research, propulsion system modeling, and performance prediction applications.

The UIUC Propeller Database encompasses two primary categories of information: propeller geometry parameters including basic design specifications such as diameter, number of blades, and pitch; and performance data comprising key metrics such as thrust coefficient C_T, power coefficient C_P, and efficiency η measured across different rotational speeds and forward velocities.

Within the UIUC database, multiple performance datasets are recorded for each propeller type at various rotational speeds. For illustrative purposes, Table 3 presents partial performance data for the 6 propeller operating at 3040 RPM, demonstrating the typical data structure and parameter relationships available in the database.

The UIUC Propeller Database provides valuable benchmark data for static performance modeling. However, when using it for model validation, its limitations should be noted: (1) The data are all measured under uniform inflow and static conditions, lacking dynamic inflow or unsteady aerodynamic effects present in real flight; (2) The database primarily covers a specific brand (APC) series of propellers, with a limited range of geometric types; (3) The data do not provide structural material information of the propellers. Therefore, the validation based on the UIUC database in this paper primarily demonstrates the model's interpolation and extrapolation capabilities within static, uniform flow fields and a limited range of geometric variations. The model's performance in more complex dynamic environments or with entirely new propeller geometries requires further validation through the test rig and the flight tests .

Table 3. APC 12 × 6 3040 rpm Performance Data.

J	C_T	C_P	Eta
0.151095	0.080788	0.032338	0.377474
0.191688	0.073512	0.031502	0.447322
0.229924	0.065819	0.029895	0.506223

3.3. Simplified Inflow Testing Rig

Publicly available motor datasets frequently lack propeller inflow data, with corresponding pitch and thrust measurements rarely documented. To address this limitation and further validate the model's applicability beyond publicly available propeller data, this study employed a custom-designed simplified inflow testing rig to collect comprehensive data for various propellers and motors under controlled inflow conditions (horizontal direction, constant velocity). Figure 2 illustrates the physical configuration of the simplified inflow testing apparatus.

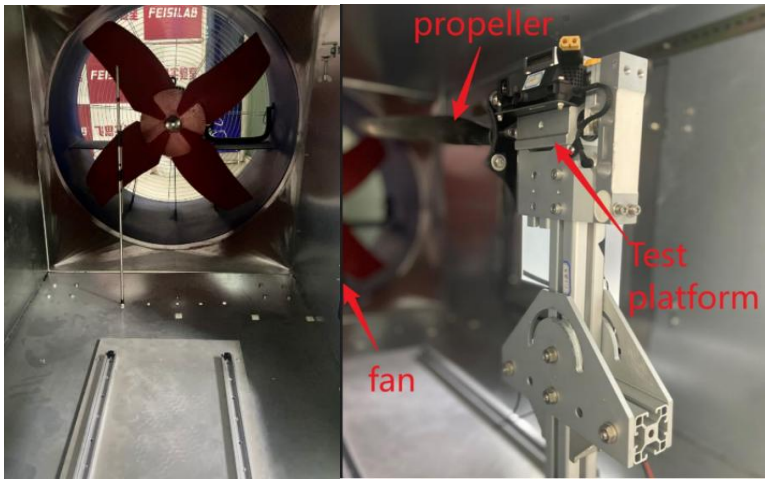


Figure 2. Schematic diagram of the simplified inflow testing rig used for experimental validation under controlled airflow conditions.

The simplified inflow testing rig enables acquisition of multiple critical test parameters: motor parameters including voltage U, current I, rotational speed n, and output power P_M; propeller parameters comprising thrust T, torque Q, and power P_P; and supplementary parameters such as air inflow velocity V_{air} and propeller pitch angle θ.

Critical mechanical quantities (thrust T and torque Q) as well as electrical parameters (voltage U, current I) are synchronously acquired through an integrated six-component test stand. The key sensors used in this test stand have the following specifications:

- Force sensor: Range 10 kg, accuracy ±0.1% F.S. ±20 g, resolution 0.001 kg.
- Torque sensor: Range 5 N·m, accuracy ±0.2% F.S. ±0.01 N·m, resolution 0.001 N·m.
- Voltage/Current sensor: Voltage range 8–80 V, accuracy ±0.05% ± 0.05 V; Current range 0.1–80 A, accuracy ±0.4% ± 0.1 A.
- Rotational speed sensor: Range 1500–300,000 RPM, accuracy ±0.5% ± 10 RPM.

Within the measurement ranges involved in this study (e.g., thrust typically less than 5 kg and torque less than 2 N·m), the systematic errors of the above sensors are far smaller than the typical variation amplitude of the measured signals. Therefore, the measurement uncertainty they introduce has a negligible impact on the model validation results.

While the simplified inflow testing rig presents certain limitations compared to large-scale wind tunnel facilities—particularly in its capability to provide only horizontal inflow and generate limited wind speed ranges—it offers significant advantages in terms of experimental space requirements and implementation portability. Given that this study does not involve complex wind field conditions, the simplified inflow testing rig adequately satisfies fundamental experimental requirements while providing practical benefits for rapid prototyping and validation.

It is important to acknowledge the limitations of this self-built inflow test apparatus: (1) It can only provide horizontal, approximately uniform steady flow, and cannot simulate vertical wind shear, turbulence, or dynamically varying inflow conditions that may be encountered in flight; (2) limited by motor power and apparatus size, the achievable wind speed range (0–15 m/s) is finite and does not cover all possible flight speeds.

Despite these limitations, the custom test rig provides a practical and cost-effective means to collect comprehensive propulsion system data under controlled inflow conditions. The dataset generated includes

- Propeller Aerodynamic Performance:Thrust (T) and torque (Q) measurements across a range of inflow velocities (0–15 m/s) and rotational speeds (1500–10,000 RPM) for multiple propeller geometries.
- Motor Electrical Characteristics: Current (I_e), voltage (U), and input power (P_M) profiles under varying aerodynamic loads.
- Synchronous Multi-parameter Data: Time-synchronized recordings of all mechanical and electrical parameters, enabling detailed analysis of energy conversion efficiency and dynamic responses.

For researchers without access to high-cost wind tunnels, our experimental methodology and open-source data provide a reproducible alternative for propulsion system characterization.

Therefore, validation on this apparatus primarily demonstrates the model's validity under steady, uniform inflow. The model's performance in non-uniform, unsteady flow fields requires evaluation through more comprehensive wind tunnel tests or extensive flight data.

3.4. Existing Parameter Estimation Models

Previous research efforts have extensively explored propeller performance parameter estimation based on wind tunnel performance data. Refs. [20,27] present final fitting results obtained through respective processing methodologies for propeller datasets. This section compares the model proposed in this study against these established approaches in terms of prediction accuracy.

In the following equations, the symbols $\hat{C}_T$ and $\hat{C}_P$ denote the model-predicted values of the thrust and power coefficients, respectively, distinguishing them from the actual coefficients C_T and C_P .

In [20], the polynomials employed for estimating propeller power and thrust coefficients are expressed as

$$\begin{aligned}\hat{C}_T &= 0.02791 - 0.06543J + 0.11867\beta + 0.27334\beta^2 \\ &\quad - 0.28852\beta^3 - 0.23504J^2 + 0.02104J^3 + 0.18677\beta J^2 \qquad (18)\\ \hat{C}_P &= 0.01813 + 0.00343J - 0.06218\beta + 0.35712\beta^2 \\ &\quad - 0.23774\beta^3 - 0.12350J^2 + 0.07549\beta J. \qquad (19)\end{aligned}$$

In [27], the fundamental polynomial forms for propeller thrust and power coefficients are defined as

$$\hat{C}_T(J) = b_{T2}J^2 + b_{T1}J + b_{T0}, \qquad (20)$$

$$\hat{C}_P(J) = b_{P3}J^3 + b_{P2}J^2 + b_{P1}J + b_{P0}. \qquad (21)$$

with polynomial coefficients provided through a novel empirical modeling approach.

For clarity in subsequent validation procedures, the model from [20] is designated as $Model - A$, the model from [27] as $Model - B$, while the models proposed in this study are labeled as $Model - Diff$ and $Model - Same$ for cross-model and single-model estimation scenarios respectively.

3.5. Propeller Parameter Estimation Results

For validation of propeller parameter estimation models, following the proposed modeling framework outlined in previous sections, the validation process was structured around two primary scenarios: parameter estimation for identical propeller models based on existing data, and parameter estimation for different propeller models based on existing data.

We employed a multi-source experimental dataset that combines the following:

1. UIUC Propeller Database:Comprehensive wind-tunnel measurements of C_T, C_P, and efficiency (η) across a wide range of advance ratios (J) for 17 distinct APC propeller models. These data provide the foundation for static performance modeling and cross-propeller generalization analysis.
2. Inflow Test Rig Data: Synchronous measurements of propeller thrust (T), torque (Q), power (P_P), and motor electrical parameters (I_e, U, n) under controlled horizontal inflow conditions (0–15 m/s). These data capture dynamic inflow effects essential for motor current model development and validation.

All experimental data used in this study—including the propeller performance and motor current data—have been made publicly available in our GitHub repository to ensure reproducibility and facilitate further research.

For the identical propeller model estimation case, Figure 3 presents performance parameter estimation results for C_T and C_P across four selected propeller models from the UIUC database. Quantitative assessment of estimation accuracy for thrust coefficient C_T and power coefficient C_P is provided through Root Mean Square Error (RMSE) and R-squared (R^2) deviation metrics relative to experimental data, with comprehensive results displayed in Figure 4 and Table 4.

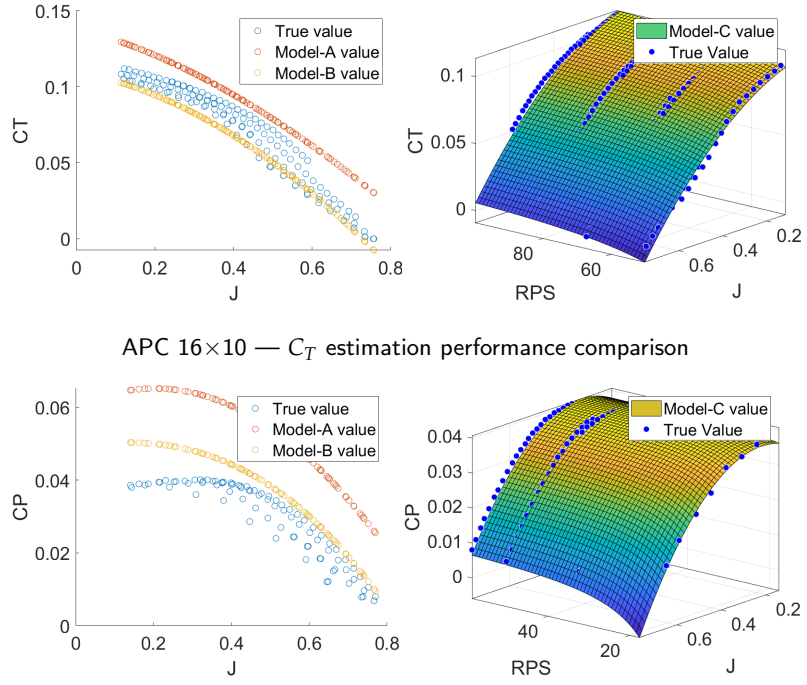


Figure 3. Performance parameter estimation results for identical propeller models, using experimental data from the UIUC Propeller Database and custom inflow tests.

The results demonstrate that the parameter estimation model proposed in this study achieves significantly reduced errors compared to models presented in [20,27]. Comparable performance prediction strategies were investigated in [30], where surrogate models calibrated through wind tunnel experiments predicted eVTOL propulsion system behavior under varying operational conditions.

The above results indicate that for identical propeller models, the model achieves extremely high prediction accuracy ($R^2 > 0.99$). This can be attributed to the following factors: (1) dimensional analysis compresses multiple physical variables into a few key

parameters (J, n^{-2}), greatly reducing the fitting dimensionality; (2) the second-order polynomial provides sufficient approximation capability for propeller aerodynamic characteristics within the selected parameter space; (3) the training data cover the main operating range of that specific propeller model. However, it should be noted that this high accuracy is achieved under the strong constraint of the "same-model". For propellers with minor geometric differences, prediction still requires the "cross-model" approach.

Table 4. Comprehensive performance metrics for four modeling approaches, highlighting superior prediction accuracy of the proposed methods across both thrust and power coefficient estimation tasks.

	$C_T - R^2 \uparrow$	$C_P - R^2 \uparrow$	$C_T - RMSE \downarrow$	$C_P - RMSE \downarrow$
$Model - A$	0.4571	−2.1878	0.0255	0.0210
$Model - B$	0.9445	0.6028	0.0078	0.0073
$Model - Diff$	0.9755	0.9346	0.0052	0.0028
$Model - Same$	0.9923	0.9906	0.0030	0.0012

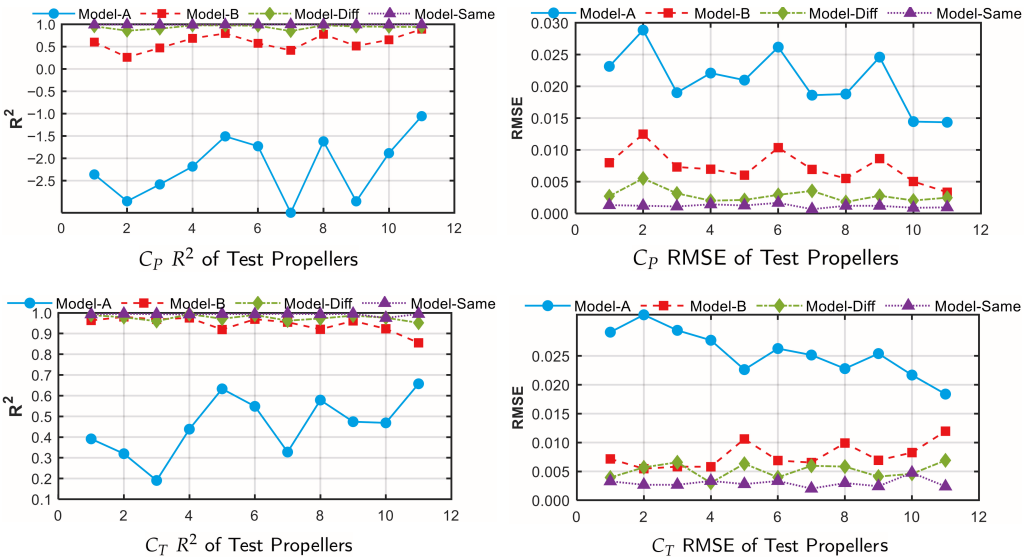


Figure 4. Comparative validation results across four modeling approaches, quantifying prediction accuracy through RMSE and R-squared metrics for thrust and power coefficient estimation.

For the different propeller model estimation scenarios, among the 17 distinct propeller models in the UIUC database, six models were selected as training data for model development, while the remaining eleven models provided test data for parameter estimation validation. Table 5 details the specific division between training and test datasets. The output results are presented in Figure 5 through scatter plot visualizations.

Table 5. UIUC dataset partition strategy for cross-model validation, ensuring representative sampling across different propeller geometries and performance characteristics.

Training/Test	**Model**
Training data	APC 12 × 6, APC 12 × 8, APC 12 × 10, APC 21 × 13, APC 13 × 10, APC 13 × 65
Test data	APC 13 × 8, APC 14 × 10, APC 14 × 7, APC 14 × 85, APC 16 × 10, APC 16 × 12, APC 16 × 8, APC 18 × 10, APC 18 × 12, APC 18 × 8, APC 20 × 10

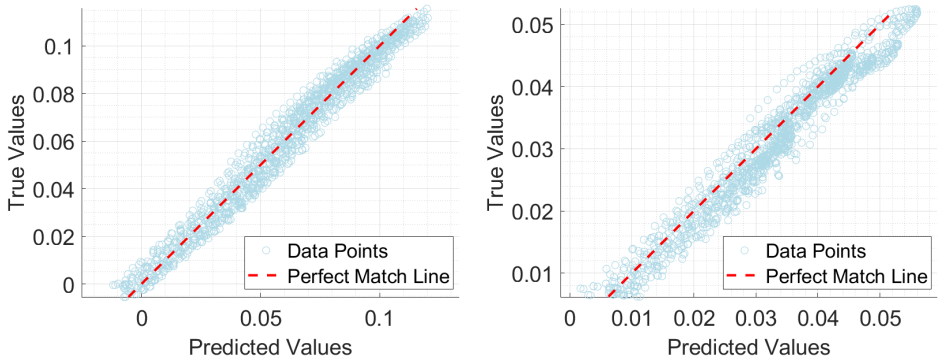


Figure 5. Cross-model propeller parameter estimation results, demonstrating model generalization capability across diverse propeller geometries not included in training datasets.

The estimation accuracy for thrust coefficient C_T and power coefficient C_P obtained from the four models is quantified through Root Mean Square Error (RMSE) metrics relative to experimental data, with comprehensive results presented in Figure 4. The results indicate that among the two models proposed in this study, while the cross-model parameter estimation approach demonstrates slightly reduced accuracy compared to the single-model estimation method, its estimation accuracy for most propeller models remains superior to the model proposed in [27] and substantially outperforms the model proposed in [20].

3.6. Motor Current Estimation Results

For validation of the motor current estimation model, five distinct motor models from various manufacturers underwent testing under zero-inflow conditions. The validation results, presented in Figure 6, demonstrate that under no-inflow conditions, minimal differences exist between prediction results from thrust-based and torque-based current prediction models, with both approaches achieving high accuracy levels.

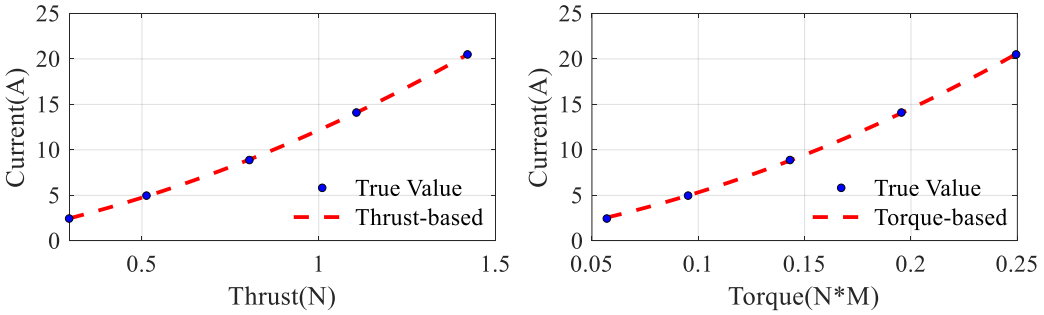


Figure 6. Motor current estimation performance for Xoar TA130-25 KV80 (XOAR International, Arcadia, CA, USA) motor under zero inflow conditions, comparing thrust-based and torque-based modeling approaches.

For inflow condition validation, data from three distinct motor models from different manufacturers were selected for comprehensive verification. Inflow condition data were collected using the simplified inflow testing rig, with the specific motor models employed in simplified inflow testing experiments detailed in Table 6.

Table 6. Motor models utilized in inflow testing experiments, representing diverse manufacturers and performance characteristics for comprehensive model validation.

Test Components	Test Models
Motor	SunnySky V3508 KV580 (SunnySky, Zhuhai, China), T-motor F100 KV1100 (T-Motor, Nanchang, China), T-motor F40 pro IV 2400kv (T-Motor, Nanchang, China)

Comprehensive datasets were collected for motors under simplified inflow conditions using the custom testing rig. The acquired dataset was subsequently applied to both modeling approaches for fitting analysis and comparative performance assessment.

As illustrated in Figure 7, while the two models exhibit minimal performance differences under zero-inflow conditions, significant disparities in motor current prediction accuracy emerge under inflow conditions. Notably, the quadratic polynomial based on torque demonstrates excellent data fitting characteristics and superior prediction accuracy, validating the theoretical advantages of torque-based modeling for dynamic operational scenarios.

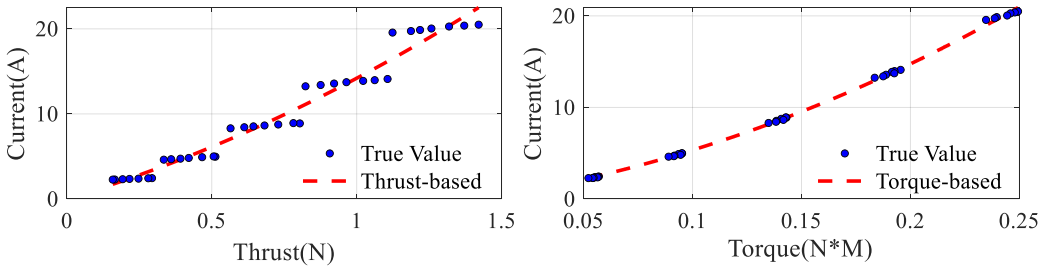


Figure 7. Motor current estimation performance for SunnySky V3508 KV580 motor under controlled inflow conditions, highlighting the superior accuracy of torque-based modeling in dynamic airflow environments.

3.7. Flight Validation

To bridge the gap between component-level prediction and system-level performance, and to directly validate model accuracy under realistic operating conditions, comprehensive flight testing was conducted. The primary objective of these flight tests focused on validating propulsion system performance model accuracy, specifically motor current prediction, during steady, level forward flight conditions. This operational scenario represents a common and critical state for numerous UAV missions.

The experimental setup employed a quadrotor platform for flight testing, with relevant system parameters measured prior to testing campaigns. Table 7 details the specific parameter values for the experimental platform. The UAV utilized in testing and the experimental flight site configuration are illustrated in Figure 8. The specific propulsion components included T5050 propellers paired with T-Motor F40 Pro II 1750kv (T-Motor, Nanchang, China) motors. Key parameters extracted from flight logs for model validation comprised motor current (I_e) as the primary electrical parameter for endurance estimation; ground speed and inflow velocity (V) derived from GPS and IMU data for advance ratio J calculation; and flight attitude parameters to ensure analysis during steady, level flight segments. Flight data were recorded by the onboard PX4 autopilot. Key state estimates were provided by its built-in sensor fusion algorithm (ESKF), with typical accuracies of the used sensors as follows:

- Current sensor: Measurement error typically $< \pm 2\%$.
- Global Navigation Satellite System (GNSS): Horizontal positioning accuracy approximately ± 1.5 m (single point), velocity accuracy approximately ± 0.1 m/s.

- Inertial Measurement Unit (IMU): Accelerometers and gyroscopes were calibrated, with attitude estimation error typically being $< \pm 2^\circ$ during steady flight.

Comparison between measured motor current and model-predicted values enables assessment of predictive capability in real-world, integrated system operations.

Table 7. Comprehensive parameter specification for quadrotor drone systems utilized in flight validation experiments.

Parameter	Numerical Values/Model
Mass	1540 g
Propeller	T5050
Motor	T-Motor F40 Pro II 1750kv
Battery	ACE 4s-5300mah
Drag Coefficient	0.51

Testing occurred in near-windless environmental conditions. Prior to each experimental trial, the UAV's maximum forward flight speeds were systematically configured at 2, 4, 6, 8, and 10 m/s sequentially through the QGroundControl (QGC) ground station interface. The UAV executed straight-line back-and-forth flight patterns within designated test areas, with flight log data recorded at high frequency to capture target parameters for subsequent post-processing analysis. To eliminate the influence of sensor noise and high-frequency vibrations, the raw current, speed, and attitude data extracted from the logs were preprocessed using a low-pass filter. Subsequent analysis focused on steady-state level flight phases.

Extracted performance metrics included flight attitude angles and real-time current draw, with the actual flight process illustrated in Figure 9.



Figure 8. Experimental UAV platform and test environment configuration for flight validation campaigns, ensuring controlled conditions for propulsion system performance assessment.

During steady-state level flight phases, under ideal operational conditions, multi-rotor UAV rotor speeds along with generated thrust and torque, together with corresponding motor current and pitch angles, achieve stable equilibrium states. Relevant flight data during steady level flight at 10 m/s is presented in Figure 9. Comparative analysis with the comprehensive model presented in [31] (utilizing model parameters: $A = 6$, $\varepsilon = 0.85$, $\lambda = 0.75$, $\zeta = 0.55$, $e = 0.83$, $C_{\mathrm{fd}} = 0.015$, $\alpha_0 = 0$, $K_0 = 6.11$) reveals current data across different forward flight speeds as displayed in Table 8. After accounting for airflow disturbances and external interference factors, the model proposed in this study demonstrates robust predictive capability for propulsion system performance under steady-state level flight conditions.

Flight validation preliminarily confirms the model's predictive capability under real flight conditions. However, the flight speed points covered in this validation (2, 4, 6, 8, 10 m/s)

and the flight mode (steady-level flight) are relatively limited. Future work requires collecting more diverse flight data, including different climb/descent rates, maneuvers, and longer-duration mission data, to comprehensively assess the model's robustness within complex, dynamic flight envelopes and the long-term cumulative effects of prediction errors.

Table 8. Comparative prediction performance between proposed torque-based modeling and conventional thrust-based approaches across different level flight speeds, demonstrating the superior accuracy of the torque-based method, particularly at higher velocities.

Speed	I_{Actual}	$I_{With-Airflow}$	$I_{Without-Airflow}$
2 m/s	26.8A	26.6A (0.7%)	25.1A (6%)
6 m/s	28.4A	29.3A (3%)	25.8A (7%)
10 m/s	31.6A	31.8A (0.7%)	27.3A (14%)

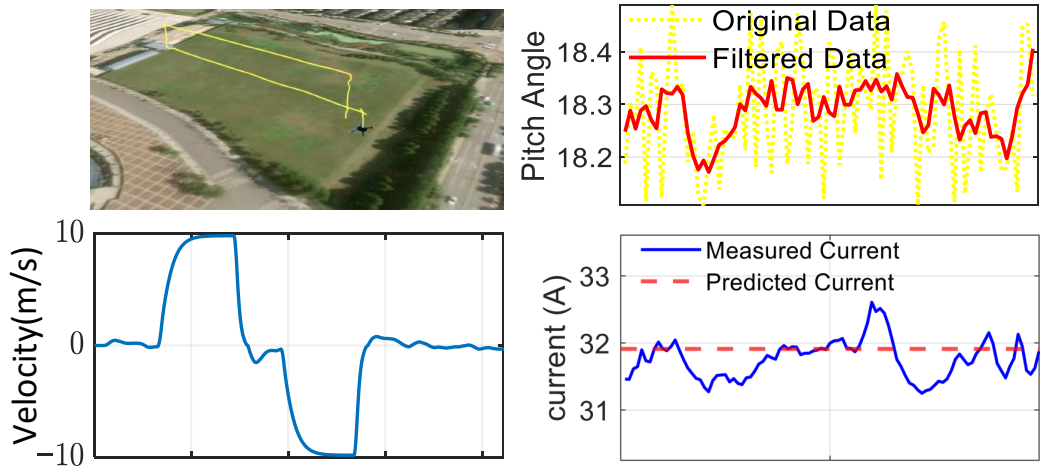


Figure 9. Flight trajectory and corresponding performance data at 10 m/s forward flight speed, illustrating stable operational conditions for model validation.

The complete model implementation and results presented in this article are publicly accessible through: https://github.com/RflySim/RflySimPropellerModel (accessed on 1 November 2025.)

4. Discussion

The validation results comprehensively demonstrate that the proposed data-driven modeling approach effectively addresses the challenges of UAV propulsion system performance prediction. The integration of dimensional analysis with polynomial regression establishes a robust framework that balances prediction accuracy with computational efficiency. The torque-based motor current model, in particular, demonstrates significant advantages under varying inflow conditions compared to traditional thrust-based approaches, validating the theoretical foundations established in the methodology development.

The successful flight validation campaigns further confirm the practical applicability of the proposed methodology in real-world UAV operational scenarios. The model's demonstrated ability to accurately predict motor current across different flight speeds highlights its potential for integration into UAV design tools and flight control systems, providing tangible benefits for mission planning and endurance estimation improvement.

Beyond the methodological innovations, this work contributes an extensive experimental dataset that bridges the gap between isolated component testing and integrated system validation. While high-fidelity wind-tunnel facilities remain inaccessible to many research

groups, our open-source dataset—combining UIUC wind-tunnel data and inflow test measurements—provides a comprehensive resource for the UAV research community. The inclusion of synchronized mechanical and electrical measurements under dynamic inflow conditions is particularly valuable, as such data are rarely available in public repositories yet are essential for accurate motor current and endurance prediction.

The systematic comparison with existing models reveals several distinct advantages of our proposed approach. The dimensionless parameter framework enables superior generalizability through cross-model prediction capabilities that outperform specialized empirical models, facilitating broader optimization searches across diverse propulsion system configurations.

Furthermore, the model achieves exceptional data efficiency by attaining high accuracy with limited training data, thereby reducing the need for extensive experimental campaigns during the optimization process and accelerating design iteration cycles. Additionally, the polynomial formulation provides computational efficiency through rapid performance evaluation suitable for design optimization loops and endurance estimation improvement, offering practical advantages for engineering applications requiring frequent performance assessments.

Although the model demonstrates high accuracy in validation, when applying it to critical missions (e.g., endurance prediction), the propagation of modeling errors should be considered. Main error sources include (1) polynomial fitting residuals, especially for predictions made outside the training data range; (2) sensor measurement noise (e.g., current, rotational speed); (3) unmodeled physical effects (e.g., viscous effects at low Reynolds numbers). These errors may accumulate in long-duration, dynamically varying missions, affecting the reliability of endurance prediction.

Additionally, the assumption of material consistency across propeller designs may restrict applicability to propellers with substantially different structural properties and manufacturing materials. Future research initiatives should focus on expanding database coverage to encompass broader geometric parameter ranges and incorporating material property effects to enhance model robustness and generalizability.

It is also important to note the limitations of the current experimental validation, particularly in the flight tests. As acknowledged in Section 3.7, the validation was conducted under a limited set of steady-level flight conditions and forward speeds. While the results are promising, a more extensive dataset encompassing diverse flight maneuvers (e.g., climbing, descending, aggressive turns) and longer mission durations is necessary to fully characterize the model's performance and error accumulation in complex, real-world operational scenarios. This expansion of the validation envelope is also a key objective for future work.

The parametric model framework proposed in this paper provides a solid foundation for integration with adaptive learning and online system identification methods. For instance, the polynomial coefficients in the model could be updated online via Bayesian updating or recursive least squares estimation using real-time flight data (e.g., real-time current, rotational speed), enabling the model to adapt to environmental changes or system degradation. Furthermore, combining this framework with model-based reinforcement learning or meta-learning could accelerate model adaptation across different UAV platforms or mission scenarios. These directions [32,33] represent important pathways for enhancing UAV intelligence and autonomy, and are significant evolution directions for this framework.

5. Conclusions

This paper presents a data-driven modeling framework for UAV electric propulsion systems that integrates dimensional analysis with empirical fitting to improve endurance es-

timation. By systematically applying the Buckingham π theorem, dimensionless parameter relationships are established, enabling accurate prediction of thrust/power coefficients (C_T, C_P) and motor current (I_e) across diverse propeller geometries and operating conditions. A novel torque-based motor current model significantly improves prediction accuracy under dynamic inflow conditions. The framework is rigorously validated against the UIUC propeller database, a custom-built inflow test rig, and actual flight tests, demonstrating superior prediction accuracy and cross-configuration generalization capability compared to existing typical methods, while maintaining computational efficiency.

Current model limitations include its dependence on the geometric parameter range of the training data, the assumption of propeller material consistency, and the deliberate exclusion of compressibility effects.

Future work will focus on expanding the open-source propeller database and enhancing the model's environmental adaptability. Specifically, ambient temperature and pressure variations, which directly affect air density and thus the advance ratio, will be incorporated into the dimensionless analysis framework to improve prediction robustness across different operational conditions. Beyond the current incompressible flow assumption, another important direction is to extend the framework for high-speed applications by accounting for compressibility effects through Mach number. Exploring transfer learning techniques will further improve the model's generalizability to novel propulsion systems and complex flight envelopes.

Author Contributions: Conceptualization, X.D., W.L. and Y.C.; Methodology, X.D., W.L. and Y.C.; Software, X.D.; Validation, X.D. and W.L.; Formal Analysis, X.D., W.L. and Y.C.; Investigation, X.D. and W.L.; Resources, Y.C.; Data Curation, X.D. and W.L.; Writing—Original Draft Preparation, X.D.; Writing—Review and Editing, X.D., W.L. and Y.C.; Visualization, X.D. and W.L.; Supervision, Y.C.; Project Administration, Y.C.; Funding Acquisition, Y.C. All authors have read and agreed to the published version of the manuscript.

Funding: This work was supported in part by the National Natural Science Foundation of China (Grant No. 62406345, 62003374), and in part by the Natural Science Foundation of Hunan Province (Grant No. 2025JJ50341).

Data Availability Statement: The data presented in this study are available in the UIUC Propeller Database and the GitHub repository: https://github.com/RflySim/RflySimPropellerModel (accessed on 1 November 2025.).

Acknowledgments: The authors would like to thank the University of Illinois at Urbana-Champaign for providing the propeller database used in this study.

Conflicts of Interest: The authors declare no conflicts of interest.

References

1. Jia, N.; Yang, Z.; Yang, K. Operational effectiveness evaluation of the swarming UAVs combat system based on a system dynamics model. *IEEE Access* **2019**, *7*, 25209–25224.
2. Santos, N.P.; Rodrigues, V.B.; Pinto, A.B.; Damas, B. Automatic Detection of Civilian and Military Personnel in Reconnaissance Missions using a UAV. In Proceedings of the 2023 IEEE International Conference on Autonomous Robot Systems and Competitions (ICARSC), Tomar, Portugal, 26–27 April 2023; IEEE: New York, NY, USA, 2023; pp. 157–162.
3. Pham, T.H.; Ichalal, D.; Mammar, S. Complete coverage path planning for pests-ridden in precision agriculture using UAV. In Proceedings of the 2020 IEEE International Conference on Networking, Sensing and Control (ICNSC), Nanjing, China, 30 October–2 November 2020; IEEE: New York, NY, USA, 2020; pp. 1–6.
4. Duarte, A.; Borralho, N.; Caetano, M. A Machine Learning Approach to Detect Dead Trees Caused By Longhorned borer in Eucalyptus Stands Using UAV Imagery. In Proceedings of the 2021 IEEE International Geoscience and Remote Sensing Symposium IGARSS, Brussels, Belgium, 11–16 July 2021; IEEE: New York, NY, USA, 2021; pp. 5818–5821.

5. Li, C.; Li, Z. Research on the use of drones for logistics distribution network terminal system based on computer 5G technology. In Proceedings of the 2022 International Conference on Electronics and Devices, Computational Science (ICEDCS), Marseille, France, 20–22 September 2022; IEEE: New York, NY, USA, 2022; pp. 441–445.
6. Sharma, S.; Kulkarni, P.; Pathak, P. Applications of unmanned aerial vehicles (UAVs) for improved business management. In Proceedings of the 2022 International Interdisciplinary Humanitarian Conference for Sustainability (IIHC), Bengaluru, India, 18–19 November 2022; IEEE: New York, NY, USA, 2022; pp. 53–57.
7. NC, A.V.; Yadav, A.R.; Mehta, D.; Belani, J.; Chauhan, R.R. A guide to novice for proper selection of the components of drone for specific applications. *Mater. Today Proc.* **2022**, *65*, 3617–3622.
8. Glauert, H. *The Elements of Aerofoil and Airscrew Theory*; Cambridge University Press: Cambridge, UK, 1983.
9. Liu, X.; Zhao, D.; Oo, N.L. Comparison studies on aerodynamic performances of a rotating propeller for small-size UAVs. *Aerosp. Sci. Technol.* **2023**, *133*, 108148.
10. Sartori, D.; Yu, W. Experimental characterization of a propulsion system for multi-rotor UAVs. *J. Intell. Robot. Syst.* **2019**, *96*, 529–540.
11. Goldstein, S. On the vortex theory of screw propellers. *Proc. R. Soc. Lond Ser. A Contain. Pap. Math. Phys. Character* **1929**, *123*, 440–465.
12. Bagai, A.; Leishman, J.G. Rotor free-wake modeling using a pseudoimplicit relaxation algorithm. *J. Aircr.* **1995**, *32*, 1276–1285.
13. Kocurek, J.D.; Tangler, J.L. A prescribed wake lifting surface hover performance analysis. *J. Am. Helicopter Soc.* **1977**, *22*, 24–35.
14. Loureiro, E.V.; Oliveira, N.L.; Hallak, P.H.; de Souza Bastos, F.; Rocha, L.M.; Delmonte, R.G.P.; de Castro Lemonge, A.C. Evaluation of low fidelity and CFD methods for the aerodynamic performance of a small propeller. *Aerosp. Sci. Technol.* **2021**, *108*, 106402.
15. Cole, J.; Krebs, T.; Barcelos, D.; Bramesfeld, G. Influence of propeller location, diameter, and rotation direction on aerodynamic efficiency. *J. Aircr.* **2021**, *58*, 63–71.
16. Chen, Z.; Liu, D.; Hou, Z.; Chen, S. Mission-Oriented Propulsion System Configuration and Whole Aircraft Redundancy Safety Performance for Distributed Electric Propulsion UAVs. *Drones* **2025**, *9*, 662.
17. Tofan-Negru, A.; Ştefan, A.; Grigore, L.Ş.; Oncioiu, I. Experimental and Numerical Considerations for the Motor-Propeller Assembly's Air Flow Field over a Quadcopter's Arm. *Drones* **2023**, *7*, 199.
18. Kedarisetty, S. Model based robust control and automation design for a micro-gravity enabling multi-rotor test bed. In Proceedings of the AIAA Scitech 2019 Forum, San Diego, CA, USA, 7–11 January 2019; p. 1171.
19. Bryant, A.H.; Walters, D.K. Developing a Small-Scale Propeller Thrust Model Using Experimentation and CFD. In Proceedings of the AIAA Scitech 2021 Forum, Virtual Event, 19–21 January 2021; p. 1307.
20. Budinger, M.; Reysset, A.; Ochotorena, A.; Delbecq, S. Scaling laws and similarity models for the preliminary design of multirotor drones. *Aerosp. Sci. Technol.* **2020**, *98*, 105658.
21. Kulanthipiyan, S.; Rajendran, P.; Raja, V. Multi-perspective investigations based design framework of an electric propulsion system for small electric unmanned aerial vehicles. *Drones* **2023**, *7*, 184.
22. Blažek, J. Leakage magnetic fields of the electriC BLDC motors of small UAV. *J. Elect. Eng* **2015**, *66*, 14–17.
23. Gabriel, D.L.; Meyer, J.; Du Plessis, F. Brushless DC motor characterisation and selection for a fixed wing UAV. In Proceedings of the IEEE Africon'11, Livingstone, Zambia, 13–15 September 2011; IEEE: New York, NY, USA, 2011; pp. 1–6.
24. Çabuk, A.S.; Sağlam, Ş.; Tosun, G.; Üstün, Ö. Investigation of different slot-pole combinations of an in-wheel BLDC motor for light electric vehicle propulsion. In Proceedings of the 2016 National Conference on Electrical, Electronics and Biomedical Engineering (ELECO), Bursa, Turkey, 1–3 December 2016; IEEE: New York, NY, USA, 2016; pp. 298–302.
25. Hasılcı, B.; Mumcu, T.V. Parameter Estimation of BLDC Motors by SVM for UAV Propulsion Systems. *Erzincan Univ. J. Sci. Technol.* **2022**, *15*, 406–419.
26. Sabanci, K. Artificial intelligence based power consumption estimation of two-phase brushless DC motor according to FEA parametric simulation. *Measurement* **2020**, *155*, 107553.
27. Kedarisetty, S.; Manathara, J.G. Novel empirical models for estimating aerodynamic coefficients of small UAV propellers. *Aerosp. Syst.* **2023**, *6*, 457–471.
28. Bae, C.H.; Min, S.G. Data-Driven Electromagnetic–Thermal Coupling Optimization of Permanent Magnet Machines for UAVs. *IEEE Trans. Transp. Electrif.* **2023**, *10*, 6473–6487.
29. Dai, X.; Quan, Q.; Cai, K.Y. Design automation and optimization methodology for electric multicopter unmanned aerial robots. *IEEE Trans. Autom. Sci. Eng.* **2021**, *19*, 2354–2368.
30. Lee, J.L.; Tyan, M.; Kwon, D.Y.; Lee, J.W. Enhanced calibration and performance prediction method for entire propulsion system of eVTOL UAV. *IEEE Trans. Transp. Electrif.* **2023**, *10*, 5735–5749.
31. Shi, D.; Dai, X.; Zhang, X.; Quan, Q. A practical performance evaluation method for electric multicopters. *IEEE/ASME Trans. Mechatronics* **2017**, *22*, 1337–1348.
32. Meng, Q.; Wang, F.; Zhao, L. Incremental policy iteration for unknown nonlinear systems with stability and performance guarantees. *arXiv* **2025**, arXiv:2508.21367.

33. Zheng, H.; Shen, L.; Tang, A.; Luo, Y.; Hu, H.; Du, B.; Wen, Y.; Tao, D. Learning from models beyond fine-tuning. *Nat. Mach. Intell.* **2025**, *7*, 6–17.

Disclaimer/Publisher's Note: The statements, opinions and data contained in all publications are solely those of the individual author(s) and contributor(s) and not of MDPI and/or the editor(s). MDPI and/or the editor(s) disclaim responsibility for any injury to people or property resulting from any ideas, methods, instructions or products referred to in the content.